The third term is

$$C(3)=-\sum_{kk't}M(k,k')(-1)^{k+t}(2t+1)^{1/2}\times\sum_j\Big([\mathbf{y}_j^{(k)}\times[\mathbf{Z}^{(k)T}\times\mathbf{w}_j^{(k')T}]^{(t)}\times\mathbf{U}^{(k')}]^{(0)}+[\mathbf{U}^{(k')}\times[\mathbf{w}_j^{(k')}\times\mathbf{Z}^{(k)}]^{(t)}\times\mathbf{y}_j^{(k)T}]^{(0)}\Big). \quad (59)$$

By calculations similar to those which led to Eq. (35) it may be shown that

$$[\mathbf{Z}^{(k)T}\times\mathbf{w}_j^{(k')T}]^{(t)}=(-1)^{k+t}[\mathbf{w}_j^{(k')T}\times\mathbf{Z}^{(k)T}]^{(t)}-(2t+1)^{1/2}\begin{Bmatrix}k & k' & t\\ l'' & l & l'\end{Bmatrix}\mathbf{y}_j^{(t)T}, \quad (60a)$$

and

$$[\mathbf{w}_j^{(k')}\times\mathbf{Z}^{(k)}]^{(t)}=(-1)^{k+t}[\mathbf{Z}^{(k)}\times\mathbf{w}_j^{(k')}]^{(t)}-(2t+1)^{1/2}\begin{Bmatrix}k & k' & t\\ l'' & l & l'\end{Bmatrix}\mathbf{y}_j^{(t)}. \quad (60b)$$

Since we have already seen that the contribution of $\mathbf{Z}^{(k)T}$ vanishes when this operator acts on a configuration where the l' shell is filled, and the same holds for $\mathbf{Z}^{(k)}$ acting on the left on such a configuration, we get

$$C(3)=\sum_{kk't}M(k,k')(-1)^{k+t}(2t+1)\times\begin{Bmatrix}k & k' & t\\ l'' & l & l'\end{Bmatrix}\sum_j\Big([\mathbf{y}_j^{(k)}\times\mathbf{y}_j^{(t)T}\times\mathbf{U}^{(k')}]^{(0)}+[\mathbf{U}^{(k')}\times\mathbf{y}_j^{(t)}\times\mathbf{y}_j^{(k)T}]^{(0)}\Big)$$
$$=2\sum_{kk't}M(k,k')(-1)^{k+t}(2t+1)\times\begin{Bmatrix}k & k' & t\\ l'' & l & l'\end{Bmatrix}\begin{Bmatrix}k & k' & t\\ l & l'' & l\end{Bmatrix}(\mathbf{U}^{(k')}\cdot\mathbf{U}^{(k')})$$
$$=2\sum_{kk'}M(k,k')\begin{Bmatrix}l & l & k'\\ l' & l'' & k\end{Bmatrix}(\mathbf{U}^{(k')}\cdot\mathbf{U}^{(k')}). \quad (61)$$

The expressions of $C(1)$ and $C(2)$ agree with those of Rajnak and Wybourne; the expression of $C(3)$ agrees only if the sign of $N\delta(\Psi,\Psi')/[l]$ is changed to plus, and the whole expression (37) is multiplied by 2.

ACKNOWLEDGMENT

We would like to express our thanks to Professor J. M. Blatt for his helpful comments and his invaluable help in the preparation of the manuscript.

PHYSICAL REVIEW VOLUME 156, NUMBER 1 5 APRIL 1967

Hyperfine Structure of Nine Levels in Two Configurations of V^{51}. I. Experimental*

W. J. Childs and L. S. Goodman
Argonne National Laboratory, Argonne, Illinois
(Received 2 November 1966)

The hyperfine structure of the $3d^34s^2\ {}^4F_{3/2,5/2,7/2,9/2}$ and $3d^4(^5D)4s\ {}^6D_{1/2,3/2,5/7,7/2,9/2}$ levels in V^{51} has been studied in detail by the atomic-beam magnetic-resonance technique. Evidence of substantial J mixing within each multiplet is found. This paper discusses the experiment itself; the following paper discusses the theoretical considerations, corrections to the raw data, and the final results.

I. INTRODUCTION

ATOMIC ground-state hyperfine-structure (hfs) studies have been made for many atoms in recent years, and values of the nuclear moments have been extracted from the data. While these studies are of great value, their interpretation is not always so simple as it might appear. In particular, the composition of the atomic state (which must be known for the extraction of nuclear moments) is difficult to estimate reliably unless several states of the same configuration are examined and compared. In the case of the nuclear electric-quadrupole moment, measurement in several states of at least two different configurations is desirable.

An attractive atom from this point of view is V^{51}, which has a nuclear spin of $\frac{7}{2}$. Because of the low Z, the $3d$ electrons involved in the low even-parity configurations behave nonrelativistically, and the departure from the LS limit is very small. For the purposes of the present experiment, the $3d^34s^2\ {}^4F_{3/2,5/2,7/2,9/2}$ and $3d^44s\ {}^6D_{1/2,3/2,5/2,7/2,9/2}$ levels were sufficiently populated by thermal excitation alone.

The principal results of the investigation are, in addition to the many hyperfine-interaction constants and electronic g factors measured, the value of the ground-state nuclear electric-quadrupole moment as

* Work performed under the auspices of the U. S. Atomic Energy Commission.

determined in two different electronic configurations, and the associated differential Sternheimer effect between the two configurations. The large body of numerical results obtained is remarkably consistent with the theory.

Two sources of difficulty deserve special mention. In the early stages of gathering the data, there frequently was confusion because of the very large number of observable transitions—about 100 distinct, field-dependent $\Delta F=0$ resonances at any given value of the C field. In addition, a considerable degree of mixing among members of each multiplet (caused by the hyperfine and Zeeman operators) led to both experimental and theoretical difficulties.

II. THEORY OF THE EXPERIMENT

The atomic-beam magnetic-resonance technique of Rabi and Zacharias[1] is now so familiar as to require little comment. In effect, at the magnetic field H, the energy separation $h\nu$ of two states $|SLJIFM\rangle$ and $|SLJIF'M'\rangle$ is detected by noting an increase in the number of atoms arriving at a detector as the applied radiofrequency f passes through the resonance value ν. The rf frequency ν and field H are then recorded.

The Hamiltonian normally used in interpreting the hfs of a fine-structure state $|SLJ\rangle$ is given[2] by

$$\mathcal{H}=A_J\mathbf{I}\cdot\mathbf{J}+B_JQ_{\rm op}+C_J\Omega_{\rm op}+g_J\mu_0H(J_z+\gamma I_z),$$

where A_J, B_J, and C_J are the magnetic-dipole, electric-quadrupole, and magnetic-octupole hyperfine-interaction constants, respectively, g_J is the electronic g factor, $\mathbf{I}$ and $\mathbf{J}$ are the nuclear and electronic angular momentum operators, γ is the ratio of the nuclear to the electronic g factor, H is the external magnetic field, the quantities $\langle FM|Q_{\rm op}|FM\rangle$ and $\langle FM|\Omega_{\rm op}|FM\rangle$ are defined in the appendix of the following paper, and μ_0 is the Bohr magneton. While this Hamiltonian is sufficient for the hfs of a state of pure SLJ, it will not predict the J dependence of the hfs constants for the members of a multiplet, nor will it account for hyperfine mixing within a multiplet. The hyperfine substates are labeled by the quantum numbers F, M, where $\mathbf{F}=\mathbf{I}+\mathbf{J}$ and M is the magnetic quantum number associated with the total angular momentum $\mathbf{F}$ of the atom.

III. PROCEDURE

The experimental procedure is first to observe transitions of the type $\Delta F=0$ at small H, where the resonance frequency (which is nearly independent of A, B, and C near $H=0$) can be estimated from the optically determined value of g_J.[3] These transitions are then observed at successively larger and larger field where their resonance frequencies depend more and more strongly on A, B, and C as well as on g_J. (The nuclear g factor g_I for V^{51} is known from NMR studies.[4]) A computer optimization program, modified from one kindly supplied by Professor H. A. Shugart, is then used to find preliminary values of A, B, C, and g_J that give a best least-squares fit to all the $\Delta F=0$ data for the particular state J. This information is then used to predict the resonance frequencies for the $\Delta F=1$ transitions (which depend very strongly on A, B, and C) at small field. When these have been observed, accurate values of A, B, and C can be extracted. The best values of the parameters A, B, C, and g_J are normally obtained by a simultaneous least-squares fit to all the data. Values of the nuclear moments may then be determined from the measured values of the hyperfine-interaction constants if the composition of the atomic state is known.

TABLE I. The low levels of V I. The relative intensity of a transition between magnetic substates is proportional to the Boltzmann factor, which is given (normalized to 100 for the ground state) in the last column for a temperature of about 2040°C.

Configuration	State	Excitation energy (cm^{-1})	Normalized Boltzmann factor
$3d^34s^2$	$^4F_{3/2}$	0	100
	$^4F_{5/2}$	138	92
	$^4F_{7/2}$	323	82
	$^4F_{9/2}$	553	71
$3d^4(^5D)4s$	$^6D_{1/2}$	2112	27
	$^6D_{3/2}$	2153	26
	$^6D_{5/2}$	2220	25
	$^6D_{7/2}$	2311	24
	$^6D_{9/2}$	2424	22
$3d^4(^5D)4s$	$^4D_{1/2}$	8412	0.5

The ground term in V I is[3] $3d^34s^2\,{}^4F$, comprising the four levels $^4F_{3/2}$ (the atomic ground state), $^4F_{5/2}$, $^4F_{7/2}$, and $^4F_{9/2}$. The next term is $3d^4(^5D)4s\,{}^6D$, at about 2000 cm^{-1}, which contains the five levels with $J=\frac{1}{2}$, $\frac{3}{2}$, $\frac{5}{2}$, $\frac{7}{2}$, and $\frac{9}{2}$. These are the nine levels whose hfs is investigated in the present experiment. The next term lies above 8400 cm^{-1} and cannot at present be sufficiently populated for investigation. This information is summarized in Table I, which gives the excitation energy and the relative intensity for any hyperfine transition between magnetic substates of these low levels in V I.

IV. APPARATUS

The atomic-beam magnetic-resonance apparatus used is a conventional "flop-in" machine of the Rabi-Zacharias type[1] and has been fully described before.[5]

[1] I. I. Rabi, J. R. Zacharias, S. Millman, and P. Kusch, Phys. Rev. 53, 318 (1938); J. R. Zacharias, *ibid.* 61, 270 (1942).

[2] N. F. Ramsey, *Molecular Beams* (Oxford University Press, New York, 1956), p. 272.

[3] *Atomic Energy Levels*, edited by C. E. Moore, Natl. Bur. Std. (U. S.) Circ. No. 467, (U. S. Government Printing and Publishing Office, Washington, D. C., 1949), Vol. 1, p. 292.

[4] With the sign convention of Ref. 2, $g_I=-\mu_I/I$. A listing of various measurements of μ_I is given by G. H. Fuller and V. W. Cohen, Appendix 1 to *Nuclear Data Sheets*, compiled by K. Way *et al.* (Printing and Publishing Office, National Academy of Science—National Research Council, Washington 25, D. C., 1965).

[5] W. J. Childs, L. S. Goodman, and D. Von Ehrenstein, Phys. Rev. 132, 2128 (1963).

TABLE II. Summary of the observations on $\Delta F=0$ transitions. The labels identifying the transitions are listed in Table IV. The calculated frequencies used in the last column are for the A, B, C values that best fit the $\Delta F=1$ data, and the g_J that best fits the $\Delta F=0$ data for each state. The calculations ignore J mixing, although it is substantial for some of the states.

Configuration	State	H (G)	Transition	Observed frequency (Mc/sec)	$\nu_{obs}-\nu_{calc}$ (kc/sec)
$3d^34s^2$	$^4F_{9/2}$	10	α	10.531(8)	14
			β	10.859(8)	2
			δ	12.155(10)	3
		20	α	21.087(8)	9
			β	21.763(8)	−8
		45	α	47.678(8)	4
			β	49.313(8)	6
		70	α	74.562(8)	13
			β	77.229(8)	19
			γ	80.977(10)	9
		120	α	129.156(8)	12
		200	α	218.870(14)	−20
			β	228.562(10)	0
			γ	241.828(10)	−10
			δ	259.880(13)	−16
			ϵ	282.192(15)	+2
	$^4F_{7/2}$	10	β	8.692(10)	0
		20	β	17.450(13)	0
		30	α	26.207(10)	19
			γ	26.350(13)	−6
		50	α	43.897(8)	19
		100	α	88.927(8)	12
			β	89.877(10)	3
			γ	90.842(10)	2
			δ	90.150(10)	−11
		200	α	182.507(12)	−5
			β	186.505(14)	−2
			γ	191.031(10)	0
			δ	190.724(13)	−9
		400	β	402.777(18)	5
			γ	432.057(15)	−6
	$^4F_{5/2}$	10	α	6.017(13)	9
			β	5.573(13)	36
		20	α	12.066(8)	17
			β	11.144(8)	20
		50	α	30.377(10)	6
			β	28.204(7)	9
			γ	24.270(10)	12
		150	α	93.624(8)	8
			β	88.431(8)	3
			γ	77.958(8)	−6
		300	α	194.835(15)	28
			β	188.612(13)	−6
			γ	171.810(12)	−32
	$^4F_{3/2}$	60	α	10.073(5)	2
		100	α	16.856(12)	−2
			β	11.385(7)	18
		200	α	34.074(12)	−11
			β	23.330(5)	16
		400	α	69.633(15)	−27
			β	49.011(6)	31
		593.104	α	105.395(5)	−52
			β	76.092(5)	50
$3d^4(^5D)4s$	$^6D_{9/2}$	10	α	12.279(11)	13
		20	α	24.576(9)	10
			β	25.379(9)	15
			γ	26.567(13)	22
		40	α	49.276(11)	9
			β	50.907(10)	5
			δ	56.904(10)	−20
		60	α	74.100(7)	−2
			β	76.618(10)	3
		100	α	124.184(10)	5
			β	128.570(15)	−6
			γ	134.800(15)	−3
			δ	143.696(8)	5
		200	α	251.771(14)	2
			β	261.684(11)	−5
			γ	275.345(11)	9
$3d^4(^5D)4s$	$^6D_{9/2}$	200	δ	293.653(7)	−8
			ϵ	313.119(9)	−4
		300	α	382.872(15)	10
			β	399.660(10)	10
			γ	422.677(10)	−2
			δ	453.897(10)	−3
			ϵ	491.482(10)	−6
	$^6D_{7/2}$	10	β	11.155(10)	10
		20	β	22.372(20)	11
		40	α	44.840(8)	0
			β	45.006(8)	4
		60	α	67.562(11)	3
			β	67.932(8)	7
			γ	68.287(7)	5
			δ	67.996(9)	14
		100	α	113.603(6)	8
			β	114.630(7)	11
			γ	115.642(7)	5
			δ	114.874(10)	12
		200	α	232.203(5)	−5
			β	236.428(10)	5
			γ	240.990(9)	8
			δ	239.447(8)	19
		300	δ	384.155(18)	17
		400	α	484.920(12)	−50
	$^6D_{5/2}$	10	α	9.713(9)	10
			β	8.956(11)	7
			γ	7.622(20)	3
		15	γ	11.494(12)	5
		20	α	19.497(10)	17
			β	18.052(12)	40
		40	α	39.262(8)	3
			β	36.485(7)	3
			γ	31.447(10)	11
		60	α	59.337(12)	1
			β	55.416(7)	7
			γ	48.105(8)	12
		100	α	100.383(10)	−6
			β	94.640(8)	3
			γ	83.246(10)	24
		200	α	208.288(9)	−19
			β	200.905(8)	11
			γ	182.022(5)	30
		400	α	447.607(10)	−50
			β	453.220(10)	−7
			γ	458.738(10)	14
	$^6D_{3/2}$	10	α	7.896(9)	3
		15	α	11.892(9)	10
		20	α	15.893(20)	−5
		30	α	24.015(4)	0
		40	α	32.237(8)	−8
		60	α	49.023(9)	−22
		100	α	83.992(10)	−37
			β	61.095(10)	38
		200	α	179.781(5)	−55
			β	140.927(6)	76
		400	α	410.342(8)	−138
			β	379.563(9)	152
	$^6D_{1/2}$	5	α	2.934(12)	0
		10	α	5.913(10)	4
		20	α	11.977(10)	−5
		30	α	18.219(6)	−6
		40	α	24.637(8)	−8
		50	α	31.232(6)	−16
		75	α	48.575(12)	−23
		100	α	67.202(3)	−39
		200	α	157.222(5)	−45
		400	α	443.638(8)	67

The oven in which the vanadium metal was evaporated was placed inside a tantalum jacket which was heated by electron bombardment. The oven itself, of stabilized ZrO, could usually be heated and cooled 2 or 3 times before it required replacement.

The detector has also been described in detail.[5] In brief, the atomic beam is bombarded by a dense beam of electrons and the V^{51} ions produced are drawn off and accelerated to a magnetic electron multiplier. A mass spectrometer system rejects ions for which $A \neq 51$.

In searching for a resonance, the rf frequency is swept (in steps of about $\frac{1}{5}$ linewidth) through the frequency span of interest and the counts are fed to a multichannel scaler. Each time the frequency is stepped, the channel into which the counts are fed is also advanced. The output data (counting rate versus channel number) are both displayed and punched out. The procedure has recently been described in detail.[6]

Most of the observable $\Delta F = \pm 1$ transitions, all of which lie between 900 and 3300 Mc/sec, were induced with one or the other of two phase-locked voltage-tuned magnetrons which together cover the frequency span 700–4000 Mc/sec.

V. THE MEASUREMENTS

The observations of $\Delta F = 0$ and $\Delta F = 1$ transitions are summarized in Tables II and III, respectively. Data are given for 215 resonance observations on the nine states. Table IV gives the convention used for labeling the $\Delta F = 0$ transitions listed.

A computer program, based on the Hamiltonian given above, produced a least-squares fit to the $\Delta F = 1$ data

TABLE III. Summary of observations of $\Delta F = 1$ transitions. The calculated frequencies used in the last column were obtained on the assumption that no J mixing is present.

Configuration	State	H (G)	Transition	Observed frequency (Mc/sec)	$\nu_{obs} - \nu_{calc}$ (kc/sec)
$3d^3 4s^2$	$^4F_{9/2}$	1	$(8, -3 \leftrightarrow 7, -3)$	1820.147(12)	2
		2	"	1820.244(10)	−1
		1	$(7, -2 \leftrightarrow 6, -2)$	1590.997(12)	−4
		2	"	1591.102(14)	1
		1	$(6, -1 \leftrightarrow 5, -1)$	1362.500(15)	2
		2	"	1362.577(15)	1
		1	$(5, 0 \leftrightarrow 4, 0)$	1134.498(12)	2
		2	"	1134.497(12)	4
		1	$(5, 0 \leftrightarrow 4, -1)$	1135.843(13)	−6
		1	$(4, 4 \leftrightarrow 3, 3)$	907.559(15)	2
		1	$(4, 3 \leftrightarrow 3, 3)$	906.210(10)	2
		1	$(4, 3 \leftrightarrow 3, 2)$	907.847(12)	13
		1	$(4, 2 \leftrightarrow 3, 3)$	904.855(10)	−2
		1	$(4, 2 \leftrightarrow 3, 2)$	906.477(14)	−6
		1	$(4, 2 \leftrightarrow 3, 1)$	908.116(12)	4
		1	$(4, 1 \leftrightarrow 3, 2)$	905.124(10)	−8
		1	$(4, 1 \leftrightarrow 3, 1)$	906.753(10)	−8
	$^4F_{7/2}$	1	$(7, -3 \leftrightarrow 6, -3)$	1750.350(12)	−2
		2	"	1750.353(12)	1
		2	$(6, -2 \leftrightarrow 5, -2)$	1498.954(12)	−5
		1	$(6, -2 \leftrightarrow 5, -3)$	1499.830(7)	4
		1	$(5, -1 \leftrightarrow 4, -1)$	1248.170(15)	−12
		2	"	1248.165(15)	−15
		1	$(5, -1 \leftrightarrow 4, -2)$	1249.060(10)	11
		1	$(4, 2 \leftrightarrow 3, 2)$	997.927(10)	4
		1	$(4, 1 \leftrightarrow 3, 2)$	997.061(11)	3
		1	$(4, 2 \leftrightarrow 3, 1)$	998.777(13)	−9
	$^4F_{5/2}$	1	$(6, -3 \leftrightarrow 5, -3)$	1928.957(10)	2
		2	"	1928.810(10)	−2
		1	$(5, -2 \leftrightarrow 4, -2)$	1606.086(12)	0
		2	"	1605.917(12)	−1
		1	$(5, -1 \leftrightarrow 4, -2)$	1606.637(10)	0
		1	$(4, 3 \leftrightarrow 3, 2)$	1284.953(15)	17
		1	$(4, 4 \leftrightarrow 3, 3)$	1285.118(15)	13
		1	$(4, -1 \leftrightarrow 3, 0)$	1283.647(15)	−18
		1	$(4, 0 \leftrightarrow 3, 1)$	1283.823(15)	−11
	$^4F_{3/2}$	1	$(5, -3 \leftrightarrow 4, -3)$	2803.119(8)	0
		0.8	$(4, -2 \leftrightarrow 3, -1)$	2238.797(7)	1
		1	"	2238.751(4)	−1
		2	"	2238.527(6)	−2
		0.8	$(4, -1 \leftrightarrow 3, -1)$	2238.883(7)	−2
$3d^3 4s^2$	$^4F_{3/2}$	1	$(4, -1 \leftrightarrow 3, -1)$	2238.862(4)	−1
		2	"	2238.750(5)	−1
		0.8	$(4, 0 \leftrightarrow 3, 0)$	2238.972(7)	−2
		1	"	2238.971(5)	−3
		2	"	2238.975(8)	0
		0.8	$(4, 1 \leftrightarrow 3, 1)$	2239.064(6)	0
		1	"	2239.089(4)	3
		1	$(4, 2 \leftrightarrow 3, 2)$	2239.201(4)	3
		1	$(4, 3 \leftrightarrow 3, 2)$	2239.309(5)	0
		1	$(4, 4 \leftrightarrow 3, 3)$	2239.423(6)	2
$3d^4(^5D)4s$	$^6D_{9/2}$	1	$(7, -2 \leftrightarrow 6, -2)$	2849.857(10)	0
		1	$(5, 0 \leftrightarrow 4, 0)$	2032.121(9)	0
		1	$(4, 2 \leftrightarrow 3, 1)$	1625.933(7)	−1
		1	$(4, 1 \leftrightarrow 3, 2)$	1622.453(11)	0
		1	$(4, 2 \leftrightarrow 3, 3)$	1622.133(10)	3
	$^6D_{7/2}$	1	$(7, -3 \leftrightarrow 6, -3)$	2677.544(10)	−1
		1	$(6, -2 \leftrightarrow 5, -2)$	2294.438(11)	7
		1	$(5, -1 \leftrightarrow 4, -1)$	1911.600(11)	−1
		1	$(5, -1 \leftrightarrow 4, -2)$	1912.702(10	−11
		1	$(4, 2 \leftrightarrow 3, 2)$	1529.004(20)	−2
		1	$(4, 1 \leftrightarrow 3, 2)$	1527.902(9)	6
	$^6D_{5/2}$	1	$(6, -3 \leftrightarrow 5, -3)$	2238.062(13)	−8
		1	$(6, -3 \leftrightarrow 5, -4)$	2238.965(10)	5
		1	$(5, -2 \leftrightarrow 4, -3)$	1867.878(10)	0
		1	$(4, 0 \leftrightarrow 3, 0)$	1495.295(13)	−23
		1	$(4, 4 \leftrightarrow 3, 3)$	1496.916(13)	29
		1	$(4, -1 \leftrightarrow 3, 0)$	1494.557(15)	−7
		1	$(4, 2 \leftrightarrow 3, 3)$	1495.386(8)	3
	$^6D_{3/2}$	1	$(5, -3 \leftrightarrow 4, -3)$	2021.447(15)	3
		2	"	2020.659(15)	−3
		1	$(4, -1 \leftrightarrow 3, -1)$	1624.210(13)	1
		2	$(4, 0 \leftrightarrow 3, 0)$	1624.738(13)	4
		1	$(4, 2 \leftrightarrow 3, 2)$	1625.777(11)	−2
		1	$(4, 3 \leftrightarrow 3, 2)$	1626.295(11)	−5
		1	$(4, 4 \leftrightarrow 3, 3)$	1626.827(9)	3
	$^6D_{1/2}$	1	$(4, -3 \leftrightarrow 3, -2)$	3003.000(12)	5
			$(4, -2 \leftrightarrow 3, -3)$		
		1	$(4, 0 \leftrightarrow 3, 0)$	3005.905(20)	−10

[6] W. J. Childs and L. S. Goodman, Phys. Rev. **148**, 74 (1966).

TABLE IV. Convention for labeling $\Delta F=0$ transitions. The table applies to states of the specified J value for either configuration.

J	Transition $(F, m_F \leftrightarrow F', m_F')$	Label
$\frac{9}{2}$	$(8, -3 \leftrightarrow 8, -4)$	α
	$(7, -2 \leftrightarrow 7, -3)$	β
	$(6, -1 \leftrightarrow 6, -2)$	γ
	$(5, 0 \leftrightarrow 5, -1)$	δ
	$(4, 1 \leftrightarrow 4, 0)$	ϵ
$\frac{7}{2}$	$(7, -3 \leftrightarrow 7, -4)$	α
	$(6, -2 \leftrightarrow 6, -3)$	β
	$(5, -1 \leftrightarrow 5, -2)$	γ
	$(4, 0 \leftrightarrow 4, -1)$	δ
$\frac{5}{2}$	$(6, -3 \leftrightarrow 6, -4)$	α
	$(5, -2 \leftrightarrow 5, -3)$	β
	$(4, -1 \leftrightarrow 4, -2)$	γ
$\frac{3}{2}$	$(5, -3 \leftrightarrow 5, -4)$	α
	$(4, -2 \leftrightarrow 4, -3)$	β
$\frac{1}{2}$	$(4, -3 \leftrightarrow 4, -4)$	α

by varying the hyperfine-interaction constants for each of the nine states. For the $J=\frac{1}{2}$ state, B and C must both be 0. For the $J=\frac{3}{2}$ states, only two independent $\Delta F=1$ hyperfine intervals were measured. For the $J=\frac{9}{2}$, $\frac{7}{2}$, and $\frac{5}{2}$ states in each configuration, C is found to be zero within experimental error. It was therefore assumed to be zero for $J=\frac{3}{2}$ also, and only A and B were varied to fit the two intervals. The difference between the observed value of the resonance frequency and the value calculated from the best-fit values of A, B, and C are given in the last column of Table III for each $\Delta F=1$ transition observed.

Once the best-fit values for A, B, and C for each state had been determined from the $\Delta F=1$ data, they were used to calculate a least-squares fit to the $\Delta F=0$ resonance frequencies. For this fit, only g_J was permitted to vary for each state. The differences between the observed and calculated resonance frequencies for the $\Delta F=0$ transitions are given in the last comumn of Table II. The large residuals, particularly for $J=\frac{3}{2}$ and $\frac{1}{2}$ at large H, originate in the high degree of mixing (due to both the hyperfine and Zeeman interactions) among the states of each multiplet. The appropriate corrections will be discussed in the following paper.

$^4F_{9/2,7/2}$ and $^6D_{9/2,7/2}$ States

Because $I=\frac{7}{2}$ for V^{51}, the resonance frequencies for transitions α, β, γ, and δ in the $J=\frac{7}{2}$ states are nearly identical until moderate values of the field are reached. This caused no difficulty, and observations on the $J=\frac{9}{2}$ and $\frac{7}{2}$ states proceeded smoothly. The resonance frequency for each $\Delta F=0$ transition could be accurately predicted from observations at lower fields, except for some J mixing in the $^6D_{7/2}$ state at the largest fields. The rough values of A, B, and C found from the $\Delta F=0$ data for these four states were sufficient to make possible observations of the $\Delta F=1$ transitions.

$^4F_{5/2}$ and $^6D_{5/2}$ States

The degree of J mixing for the $J=\frac{5}{2}$ states is somewhat larger than for the $J=\frac{9}{2}$ and $\frac{7}{2}$ states, as can be seen from the larger number of residuals that exceed the probable error. Nevertheless, the $\Delta F=1$ transitions were observed near the frequencies predicted from the $\Delta F=0$ data.

The $F=6 \leftrightarrow 5$ hyperfine interval in the $^6D_{5/2}$ state lies very near the $F=4 \leftrightarrow 3$ interval in the $^4F_{3/2}$ state and was at first missed. Figure 1 shows the appearance of the series of $^4F_{3/2}$ lines $(4, M \leftrightarrow 3, M)$ for $M=-2$, -1, 0, 1 as observed at 1 G. The third line was not only surprisingly stronger than the others, but also much wider. It was subsequently found, by varying the magnetic field very slightly, that this line also includes the $^6D_{5/2}(6, -3 \leftrightarrow 5, -4)$ transition.

$^4F_{3/2}$ State

Although the gyromagnetic ratio of the $^4F_{3/2}$ state is only about $g_J=0.4$, it was found possible to deflect such atoms sufficiently to observe the usual transitions. The $\Delta F=0$ transitions in the $^4F_{3/2}$ state were observed at fields up to 593 G in order to reduce the uncertainty in the extracted values of A and B. The computer program gave a good fit (low χ^2) to all the data and predicted the hyperfine intervals $F=4 \leftrightarrow 3$ and $F=5 \leftrightarrow 4$. The first was not difficult to find because it consisted of seven lines covering a spread of frequencies at nonzero field, but the $F=5 \leftrightarrow 4$ interval could not be found in the expected neighborhood. The computer then fitted the observed $F=4 \leftrightarrow 3$, $\Delta F=1$ resonance and the $\Delta F=0$ data simultaneously. While the fit was excellent, the value $B(^4F_{3/2})=29.3\pm1.7$ Mc/sec deduced is ten times the value expected theoretically from a comparison with the results for the $^4F_{9/2,7/2,5/2,}$ states. A careful search for the $F=5 \leftrightarrow 4$ transition in a large region centered on the value deduced in this calculation also failed to reveal a resonance. At this point all the $\Delta F=0$ data were disregarded, and the $F=5 \leftrightarrow 4$ hyperfine interval was estimated from the experimental value of the $F=4 \leftrightarrow 3$ interval and the value of $B(^4F_{3/2})$ which was calculated by applying the theoretical J dependence of B to the measured B values for the $^4F_{9/2,7/2,5/2}$ states. The $F=5 \leftrightarrow 4$ transition was observed near this predicted frequency but, as can be seen from Table II, no value of g_J will reconcile the $\Delta F=0$ observations with the A and B values required by the $\Delta F=1$ observations. This is still the case if the observed A and B factors are corrected for the effects of off-diagonal hyperfine interactions, since the $\Delta F=0$ transitions are also affected by the off-diagonal matrix elements of the Zeeman operator $\mathbf{L}+2\mathbf{S}$.

$^6D_{3/2}$ State

The degree of admixture in the $^6D_{3/2}$ state, which lies only 40 cm^{-1} from the $^6D_{1/2}$ level, is somewhat greater

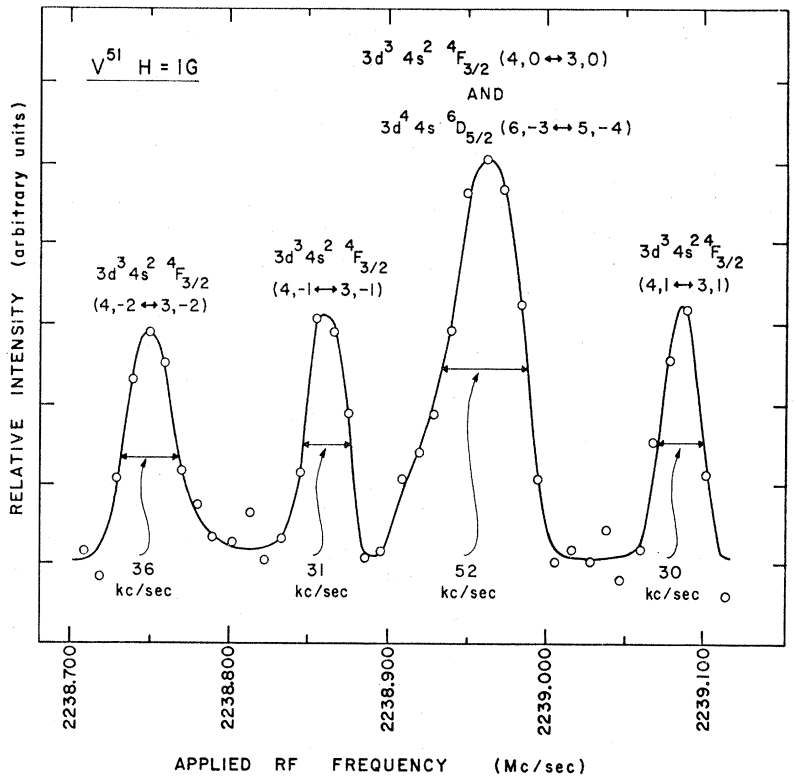

FIG. 1. Intermingling of the $\Delta F=1$ transitions $3d^3 4s^2\ {}^4F_{3/2}$, $F=4\leftrightarrow 3$ and the $3d^4(^5D)4s\ {}^6D_{5/2}$, $F=6\leftrightarrow 5$ in V^{51} as observed at 1 G. A slight shift of the magnetic field in which the transitions were induced revealed the different field dependence of the two lines superimposed here.

than for the ${}^4F_{3/2}$ state since there is no ${}^4F_{1/2}$ state. For this reason, neither the $F=5\leftrightarrow 4$ nor the $F=4\leftrightarrow 3$ hyperfine interval lies near the value predicted from the $\Delta F=0$ data, and furthermore no set of parameters A, B, and g_J can account for the observed $\Delta F=0$ data.

Due to a fortunate coincidence, however, the $F=4\leftrightarrow 3$ intervals in the ${}^6D_{9/2}$ and ${}^6D_{3/2}$ states are nearly identical, and the several components of the latter were discovered by chance while observing the former at 1 G. Figure 2 shows the pattern predicted theoretically from the frequencies measured for eight of the components. The enhanced intensity predicted for several of the ${}^6D_{3/2}$ lines is due to the almost complete degeneracy of the $J=\frac{3}{2}$, $F=3$ magnetic substates. Figure 3 shows the actual appearance of two of the lines as observed at 1 G.

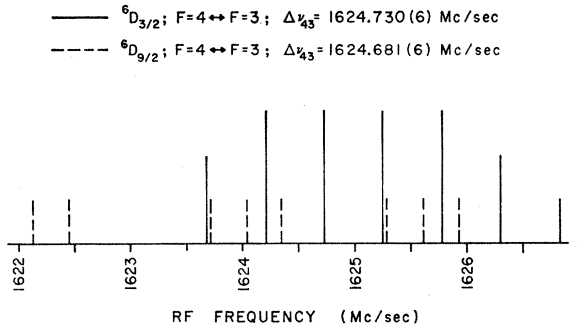

FIG. 2. Overlapping of the $F=4\leftrightarrow 3$ transitions in the states ${}^6D_{9/2}$ and ${}^6D_{3/2}$ at 1 G. The pattern was calculated from the observed resonance frequencies of eight key components out of the total of fifteen. The actual data for two of these transitions are plotted in Fig. 3. The anticipated relative intensities are proportional to the heights of the lines. The relatively greater intensities for several of the ${}^6D_{3/2}$ lines is due to the overlapping of several transitions.

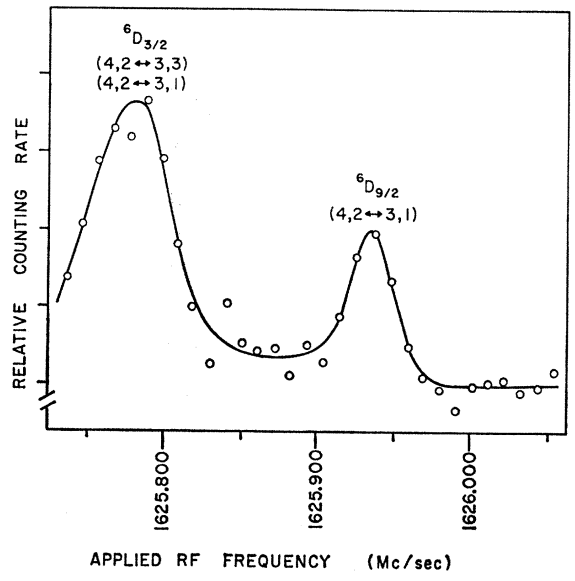

FIG. 3. Observation of $\Delta F=1$ hyperfine transitions in two different states in the same frequency sweep. Other nearby components are indicated in Fig. 2. The greater intensity observed for the ${}^6D_{3/2}$ line is caused by the overlapping of several transitions.

Since the $\Delta F=0$ data on the $^6D_{3/2}$ state are not self-consistent (when J mixing is ignored), lumping them with the observed $F=4\leftrightarrow 3$ hyperfine interval in the computer calculation will contribute nothing worthwhile. The procedure followed was the same as for the $^4F_{3/2}$ state. The value of $B(^6D_{3/2})$ was calculated theoretically from the measured values of B for the $^6D_{9/2,7/2,5/2}$ states. From this and the observed $F=4\leftrightarrow 3$ interval the $F=5\leftrightarrow 4$ interval was predicted. The transition was observed in the predicted region.

$^6D_{1/2}$ State

The degree of J mixing in the $^6D_{1/2}$ state can be expected to be substantial since it lies only 40 cm^{-1} from the $^6D_{3/2}$ state. Since J is $\frac{1}{2}$, $B=C=0$ and there are only the two parameters A and g_J. Although variation of these parameters produced an excellent fit to all $\Delta F=0$ observations through 400 G, no trace could be found of the $F=4\leftrightarrow 3$ transition within a wide band centered on the predicted frequency. The width of the region searched was about 10 times the width of the predicted region. For this level, the effects of J mixing were calculated roughly. On searching near the corrected $\Delta F=1$ prediction, we observed the $F=4\leftrightarrow 3$ transition.

It is of interest to note that $g_J\approx 3.3$ for the $^6D_{1/2}$ state. For this reason, deflection of the $^6D_{1/2}$ atoms in the inhomogeneous magnetic fields of the atomic beam apparatus was exceptionally strong.

Table V. Values of the hyperfine-interaction constants A, B, C and electronic g factors g_J found for least-squares fits to the experimental data. The values of A, B, C were obtained from fits to the $\Delta F=1$ data, and the g_J values from similar fits to the $\Delta F=0$ data using the above values of A, B, and C. The values of χ^2 for the $\Delta F=0$ fits indicate systematic differences between calculated and observed resonance frequencies for the $\Delta F=0$ transitions, particularly for $J=\frac{3}{2},\frac{1}{2}$ at high fields. The discrepancies are due to J mixing within the multiplets caused by the off-diagonal (in J) matrix elements of the hyperfine and Zeeman operators. The values given for A, B, C, and g_J are not corrected for this mixing; appropriate corrections will be discussed in the following paper.

Configuration	State	Quantity	Measured value (Mc/sec)	χ^2
$3d^34s^2$	$^4F_{9/2}$	A	227.1324(6)	
		B	7.822(15)	
		C	0.002(2)	
		g_J	1.33362(3)	15
	$^4F_{7/2}$	A	249.7398(7)	
		B	5.081(20)	
		C	−0.001(2)	
		g_J	1.23820(2)	11
	$^4F_{5/2}$	A	321.2265(12)	
		B	3.384(25)	
		C	0.000(2)	
		g_J	1.02839(3)	32
	$^4F_{3/2}$	A	560.0482(6)	
		B	4.264(8)	
		g_J	0.39899(1)	250
$3d^4(^5D)4s$	$^6D_{9/2}$	A	406.8513(16)	
		B	14.324(65)	
		C	0.006(9)	
		g_J	1.55649(2)	13
	$^6D_{7/2}$	A	382.3670(10)	
		B	2.268(29)	
		C	0.001(3)	
		g_J	1.58838(2)	25
	$^6D_{5/2}$	A	373.5180(10)	
		B	−5.459(25)	
		C	0.000(2)	
		g_J	1.65846(2)	62
	$^6D_{3/2}$	A	405.6038(12)	
		B	−8.107(12)	
		g_J	1.86851(2)	535
	$^6D_{1/2}$	A	751.4778(28)	
		g_J	3.33683(5)	144

VI. CONCLUSIONS

The least-squares fits to the observed low-field $\Delta F=1$ transitions were of high quality (low χ^2) for all nine states investigated. The values found in this way for the hyperfine interaction constants A, B, and C are listed[7] in Table V. It should be emphasized that these values have not been corrected for the effects of mixing within the multiplet by the hyperfine interactions. (These corrections are made in the following paper. They are found to be 0.01% or less for the A factors, but range up to 17% for the B factors.)

The value of g_J which, when used with the above uncorrected values of A, B, and C, gives the best least-squares fit to the observed $\Delta F=0$ transitions is also listed[7] for each state, along with the χ^2 for the fit. The χ^2 is found to be of reasonable size for the $^4F_{9/2,7/2}$ and $^6D_{9/2}$ states, slightly larger than would be expected for the $^4F_{5/2}$ and $^6D_{7/2}$ states, and very much larger than expected for the $^4F_{3/2}$ and $^6D_{5/2,3/2,1/2}$ states. The discrepancies are attributed to J mixing, and are investigated in the following paper. The values listed for g_J are thus uncorrected and are in several cases substantially in error. They are, however, the best values for use in calculations in which J mixing is ignored.

[7] Preliminary data for the two multiplets in V^{51} were published earlier by L. S. Goodman and W. J. Childs, Bull. Am. Phys. Soc. **10**, 1098 (1965) and by W. J. Childs and L. S. Goodman, *ibid.* **11**, 328 (1966). At two points there are substantial differences between these preliminary data and the results given in Table V of this paper. In the first paper, the values of A and B for the $^4F_{3/2}$ state were based on a simultaneous fit to the $\Delta F=0$ data and the observation of the $F=4\leftrightarrow 3$ transition. Although a reasonable value of χ^2 was found for this fit, the values of A and B are not consistent with the subsequent measurement of the $F=5\leftrightarrow 4$ interval. In the second paper, the preliminary values for A and g_J for the $D_{1/2}$ state were based exclusively on a fit to the $\Delta F=0$ data. As explained in the text, these data are inconsistent with the subsequently measured $F=4\leftrightarrow 3$ zero-field hyperfine interval. In each case, the apparent inconsistency vanishes when the effects of off-diagonal hyperfine and Zeeman interactions are considered. Appropriate corrections for these effects are made in the second of the present pair of papers.